Biochimica et Biophysica Acta 1840 (2014) 3145–3152

Contents lists available at ScienceDirect

Biochimica et Biophysica Acta

journal homepage: www.elsevier.com/locate/bbagen

The effect of celastrol, a triterpene with antitumorigenic activity, on conformational and functional aspects of the human 90 kDa heat shock protein Hsp90α, a chaperone implicated in the stabilization of the tumor phenotype

Letícia M. Zanphorlin, Fernanda R. Alves, Carlos H.I. Ramos *

Institute of Chemistry, University of Campinas UNICAMP, P.O. Box 6154, 13083-970 Campinas, SP, Brazil

ARTICLE INFO

Article history:
Received 27 March 2014
Received in revised form 23 May 2014
Accepted 11 June 2014
Available online 19 June 2014

Keywords:
Molecular chaperones
Hsp90
Celastrol
Protein–ligand interaction
TPR co-chaperone
Anticancer agents

ABSTRACT

Background: Hsp90 is a molecular chaperone essential for cell viability in eukaryotes that is associated with the maturation of proteins involved in important cell functions and implicated in the stabilization of the tumor phenotype of various cancers, making this chaperone a notably interesting therapeutic target. Celastrol is a plant-derived pentacyclic triterpenoid compound with potent antioxidant, anti-inflammatory and anticancer activities; however, celastrol's action mode is still elusive.

Results: In this work, we investigated the effect of celastrol on the conformational and functional aspects of Hsp90α. Interestingly, celastrol appeared to target Hsp90α directly as the compound induced the oligomerization of the chaperone via the C-terminal domain as demonstrated by experiments using a deletion mutant. The nature of the oligomers was investigated by biophysical tools demonstrating that a two-fold excess of celastrol induced the formation of a decameric Hsp90α bound throughout the C-terminal domain. When bound, celastrol destabilized the C-terminal domain. Surprisingly, standard chaperone functional investigations demonstrated that neither the in vitro chaperone activity of protecting against aggregation nor the ability to bind a TPR co-chaperone, which binds to the C-terminus of Hsp90α, were affected by celastrol.

Conclusion: Celastrol interferes with specific biological functions of Hsp90α. Our results suggest a model in which celastrol binds directly to the C-terminal domain of Hsp90α causing oligomerization. However, the ability to protect against protein aggregation (supported by our results) and to bind to TPR co-chaperones are not affected by celastrol. Therefore celastrol may act primarily by inducing specific oligomerization that affects some, but not all, of the functions of Hsp90α.

General significance: To the best of our knowledge, this study is the first work to use multiple probes to investigate the effect that celastrol has on the stability and oligomerization of Hsp90α and on the binding of this chaperone to Tom70. This work provides a novel mechanism by which celastrol binds Hsp90α.

1. Introduction

Cancer is the generic name for diseases in which abnormal cells divide without control and are invasive (malignant). According to the World Health Organization, cancer is a leading cause of death worldwide, and although important progress has been made toward its treatment, considerable research remains to be undertaken to understand the molecular basis of cancers and to identify suitable methods of treatment. There have been several studies on cancer-identified genes, later named oncogenes, which are often mutated or highly expressed in tumor cells, and many of the oncogenic proteins depend on the 90 kDa heat shock protein Hsp90 to be stable and functional (for reviews see [1–4]). As a matter of fact, Hsps are highly expressed in several cancerous tumors, most likely because they favor cell growth in stressed environments; thus, Hsps have become important targets for cancer therapy.

Hsp90 exist as homodimers (~160 kDa) in which each subunit is discretized into three domains [5–7]. The N-terminal domain contains an ATP-binding site [8] and binds natural compounds with anti-tumoral activities, such as geldanamycin (from *Streptomyces hygroscopicus*) and radicicol (also known as monorden) [9,10]. The central domain is highly charged and has a high affinity for co-chaperones and client proteins [11–13]. The C-terminal domain is essential for dimerization [14] and

Abbreviations: CD, circular dichroism; DLS, dynamic light scattering; DSC, differential scanning calorimetry; DSF, differential scanning fluorimetry; PAGE, polyacrylamide gel electrophoresis; SDS, sodium dodecyl sulfate; SEC–MALS, size-exclusion chromatography coupled to multi-angle light scattering; C-Hsp90α, C-terminal domain of Hsp90α; Hsp90α, 90 kDa heat shock protein α-isoform (paralog)

* Corresponding author. Tel.: +55 19 3521 3096; fax: +55 19 3521 3023.
E-mail address: cramos@iqm.unicamp.br (C.H.I. Ramos).

http://dx.doi.org/10.1016/j.bbagen.2014.06.008
0304-4165/

has also been demonstrated to bind compounds with anti-tumoral activities, such as cisplatin [15], novobiocin [16] and epigallocatechin-3-gallate (EGCG) [17]. It could appear counterintuitive to label an important chaperone such as Hsp90 as a cancer target, when considering its vital role in normal cells. However, cancer drugs such as 17-AAG, which inhibit Hsp90, are well tolerated by patients [18], likely because Hsp90 found in cancer cells has a much higher affinity for 17-AAG than does Hsp90 from normal cells [19,20]. Kamal et al. [19] showed that Hsp90 derived from cancer cells binds to 17-AAG up to 100 times more tightly than does Hsp90 isolated from normal cells. Hsp90 in normal cells would be in a free form while in malignant cells the chaperone would be associated with a multi-protein complex and would have a much higher ATPase activity [19,21,22]. Because cancer cells have high protein (normal and mutant) expression and live in a stressful microenvironment, they would be very dependent on Hsp90 that is in a highly activated state [3]. Other inhibitors apparently are also more effective against Hsp90 isolated from cancer cells than from normal cells [reviewed in 23]. Consequently, studies on the interaction between recombinant Hsp90 and ligands have gained increased attention worldwide, due to the potential of this chaperone as a therapeutic target for cancer [3,4,24].

Humans have two cytosolic isoforms of Hsp90, named α and β, that are highly identical [7,25]. The literature is rich in evidence that Hsp90α, which was investigated in this study, is linked to cancer and may have a diverse action than the β isoform. To mention a few examples: only Hsp90α, but not Hsp90β, has the capacity to activate oncogenic kinases [26]; Hsp90α has elevated expression in brain, skin and thyroid cancers, while Hsp90β has higher expression in bladder cancer [27]; Hsp90α is secreted by a variety of tumor cell lines, enhancing invasiveness and thus being considered a valid target for anticancer therapies (revised in [25]).

Celastrol, a quinone methide triterpene isolated from plants belonging to the family *Celastraceae* (used in Oriental medicine), has demonstrated potential anticancer activity in several cancer models, including prostate cancer, pancreatic cancer, leukemia and melanoma (See the following review and references therein: [28]). Celastrol has some action upon Hsps, the compound induces HSF-1 (heat shock factor-1) in a similar way than a heat shock treatment (42 °C) [29] and it was identified as a ligand of Hsp90 [30]. Although several investigations on the interaction of Hsp90 and celastrol have been performed, the true nature of the molecular mechanism of this chaperone-ligand interaction is still elusive. For instance, studies based on the effect of celastrol on the Hsp90–Cdc37 interaction [31] and ATPase inhibition [32,33] have suggested that celastrol binds to the N-terminal domain as this is the site of Cdc37 and ATP binding. However, trypsinolysis studies [32] suggested that celastrol binds to the C-terminal domain of the Hsp90. In addition, the targets of the celastrol in the Hsp90 complexes are still a matter of intense debate. Some studies have reported the inhibition of the Hsp90 ATPase activity by celastrol [31,33], whereas others have demonstrated no effect [31,34]. By using HSQC NMR experiments, Sreeramulu and co-workers [35] demonstrated that celastrol disrupted the Hsp90–Cdc37 complex not by binding directly to a deletion mutant of Hsp90 representing the N-terminal domain but by targeting Cdc37. Co-immunoprecipitation experiments provide conflicting results, as they have demonstrated that the Hsp90/HOP complex both could [36] and could not [31] be disrupted by celastrol.

Motivated by the need for further investigation regarding Hsp90α-celastrol interaction, we performed an extensive characterization of the interaction between them using biochemical and biophysical complementary techniques, such as size-exclusion chromatography coupled to multi-angle laser light scattering (SEC–MALS), native-PAGE, dynamic light scattering (DLS), differential scanning calorimetry (DSC), differential scanning fluorescence (DSF) and chaperone and protein–protein assays. We found that celastrol affected the oligomeric state of Hsp90α by binding to the C-terminal domain. Moreover, we report here that celastrol destabilized the C-terminus of Hsp90 but had neither an effect on the interaction of Hsp90α with its co-chaperone Tom70, which binds to the C-terminus of Hsp90α nor on the functional activity of Hsp90α against protein aggregation. To the best of our knowledge, this study is the first work to use multiple probes to investigate the effect that celastrol has on the stability and oligomerization of Hsp90α and on the binding of this chaperone to Tom70.

2. Materials and methods

2.1. Protein expression and purification

The expression and purification of the C-terminal domain of human Hsp90α (C-Hsp90α, residues 566–732) and the soluble fraction of human Tom70 (residues 111–608) were performed as previously described [37]. *Escherichia coli* strain BL21(DE3) was transformed with a pProExHta vector, in which human full-length Hsp90α was cloned and grown at 37 °C until A_{600} reached 0.8–1.0. After this step the temperature of growth was set to 18 °C, and protein expression was induced with 1.0 mM isopropyl-beta-D-thiogalactopyranoside. After overnight induction, the cells were harvested and disrupted by sonication in a buffer containing 50 mM Tris-HCl, pH 8.0, 100 mM KCl, 1 mM EDTA, 30 μg/ml lysozyme, 1 mM PMSF and 5 units DNase. The lysate was cleared by centrifugation, and the proteins were purified using nickel metal affinity chromatography (eluted by 500 mM imidazole and dialyzed afterwards) followed by size-exclusion chromatography (Superdex 200) in a buffer containing 20 mM Tris–HCl, pH 7.4, and 150 mM NaCl. Sample purity was analyzed by SDS-PAGE, and protein concentration was determined by measuring UV absorbance at 280 nm. Celastrol was kept soluble by dilution into dimethyl sulfoxide (DMSO), and the final concentration of DMSO was never higher than 2% in the experiments described below.

2.2. Circular dichroism

A JASCO model J-810 CD spectropolarimeter coupled to a thermoelectric sample temperature controller (Peltier system) was used to record circular dichroism (CD) spectra using parameters previously described [38]. Briefly, experiments were conducted with 15 μM C-Hsp90α or 10 μM of full-length Hsp90α and 9 μM Tom70 in a buffer containing 20 mM Tris–HCl, pH 7.4, and 150 mM NaCl at 20 °C. Data were collected from 260 to 200 nm using cuvettes with a 1 mm path length, and the results reported are the average of at least three experiments.

2.3. Differential Scanning Fluorescence

DSF (Differential Scanning Fluorescence) was performed using an iCycler iQ Real-Time PCR detection system with excitation and emission wavelengths of 580 and 623 nm, respectively, and monitoring with a CCD camera. Samples were 2.5 μL solutions of Sypro Orange (8×), 12.5 μL of buffer alone (control) or protein containing ligand (celastrol) and 5 μL of buffer reaction. The protein concentrations were 2 μM for either full-length Hsp90α or C-Hsp90α. Samples were added to a PCR plate with 96 wells that was sealed and heated from 20 to 90 °C. With the transition temperature of protein unfolding, Tm, a Boltzman equation was used to fit the fluorescence curve:

$$I = (A + (B\text{-}A) / (1 + \exp((Tm\text{-}T)/C)$$

where I is the fluorescence intensity at temperature T; A and B is the fluorescence intensity before and after of the transition, respectively; C is the slope of the curve [39]. DMSO (2%) was present in all samples and did not interfere with the results as confirmed by control experiments.

2.4. Differential Scanning Calorimetry

Calorimetric experiments (Differential Scanning Calorimetry) were performed using a VP-DSC calorimeter (Microcal-GE Healthcare). Proteins, 220 μM C-Hsp90α or 35 μM full-length Hsp90α, in 20 mM Tris–HCl, pH 7.4 and 150 mM NaCl were incubated with different concentrations of celastrol (see figure caption for details). Protein samples and buffers were filtered, degassed for 5 min in a vacuum system, loaded into DSC and scanned from 25 to 90 °C at a heating rate of 1.0 °C/min. Data were analyzed with GE Microcal Origin software, and baselines were calculated from both pre- and post-transition temperature regions. DMSO (0.8%) was present in all samples and did not interfere with the results, as confirmed by control experiments.

2.5. Native-PAGE

Non-denaturing polyacrylamide gel electrophoresis (native-PAGE) (pH 8.8; 12% polyacrylamide) were performed as described by Bollag et al. (1996) [40]. C-Hsp90α (23 μM) or full-length Hsp90α (12.5 μM) were incubated with celastrol at different molar ratios in a buffer containing 20 mM Tris–HCl, 150 mM NaCl pH 7.4 at 25 ºC for 10 min. 10 μL of each sample were loaded into the lanes of a 5% stacking/12% resolving gel and electrophoresed at 100 V until the dye front migrated to within 2 mm of the bottom of the gel. After electrophoresis, the gel was stained with Coomassie Blue. DMSO (2%) was present in all samples and did not interfere with the results as confirmed by control experiments.

2.6. Dynamic light scattering

Proteins (87 μM C-Hsp90α or 25 μM full-length Hsp90α) were incubated with celastrol (see figure captions for concentrations) in a buffer containing 20 mM Tris–HCl, pH 7.4, and 150 mM NaCl for 4 min and at room temperature before measurements. Dynamic light scattering (DLS) measurements were conducted on a Malvern Zetasizer Nano ZS 90 (Model No. 3690) with a 633 nm laser, in a polystyrene cell, at 25 °C and with a scattering angle of 90°. DMSO (1%) was present in all samples and did not interfere with the results as confirmed by control experiments.

2.7. Size-exclusion chromatography–multiple angle light scattering (SEC–MALS)

SEC–MALS experiments were performed using an ÄKTA FPLC instrument (GE) coupled to a triple-angle static light scattering detector miniDAWN™ TREOS (Wyatt Technology, Santa Barbara, CA, USA) at room temperature. C-Hsp90α (50 μM, dimer) in the absence or in the presence of TOM70 (100 μM) were incubated with 2- or 3-fold the concentration of celastrol (see figure captions for details) in a buffer containing 20 mM Tris–HCl, pH 7.4, and 150 mM NaCl for 2 h at 4 ºC before measurements. After incubation, 250 μL of each sample was injected into a Superdex 200 HR 10/300 GL column (GE Healthcare). Elution was performed using the same buffer, and data were processed using ASTRA V software (Wyatt Technology, Santa Barbara, CA, USA). The elution peaks were collected in 1.0 mL aliquots and assessed by Coomassie Blue-stained SDS-PAGE. DMSO (0.8%) was present in all samples and did not interfere with the results as confirmed by control experiments.

2.8. Chaperone activity

The ability of the full-length Hsp90α (4 μM) to suppress the aggregation of proteins was tested in the presence of celastrol (2-fold excess). Porcine heart citrate synthase at a 2 μM concentration was heated to 45 °C in 20 mM Tris–HCl with 150 mM NaCl, pH 7.4, in the absence or in the presence of full-length Hsp90α and celastrol (see figure caption for concentrations). Experiments were monitored by light scattering at 340 nm using a temperature-controlled *Cary* spectrofluorometer. DMSO (1%) was present in all samples and did not interfere with the results as confirmed by control experiments.

3. Results and discussion

3.1. Celastrol bound Hsp90α via the C-terminal domain with a destabilization effect

We studied the effect that celastrol, a plant-derived pentacyclic triterpenoid compound with potent anticancer activities, had on the structure and function of the human 90 kDa heat shock protein (Hsp90α), which has been implicated in the stabilization of the tumor phenotype of various cancers (for reviews see [1–4]). The effect of celastrol was tested with full-length Hsp90α, as well as with a deletion mutant (C-Hsp90α) in which only the C-terminal domain was present. The recombinant proteins were produced pure and folded as shown in Figs. S1 and S2 (Supplemental material).

Celastrol binding to Hsp90α was investigated in terms of the ability of the compound to influence the stability of the protein. The stability of a protein can be influenced by several factors such as buffer composition or the binding of a specific ligand, and it is usually and easily measured by comparing the thermal-induced unfolding profiles of the protein at different conditions. Any condition that affects the stability of a protein will affect the Gibbs free-energy of unfolding (ΔG_{unf}), the difference in free-energy between the folded and the unfolded states, and in a thermal-induced unfolding experiment, it will be measured as an increase or decrease, depending on the nature of the effect, in the midpoint of the transition (Tm) in Kelvin (or other unity, as for instance Celsius degrees) compared with the standard condition [41]. The thermal-induced unfolding of the full-length Hsp90α and C-Hsp90α were investigated by both Differential Scanning Fluorimetry (DSF) and Differential Scanning Calorimetry (DSC), and the results are summarized in Tables 1 and 2, respectively. It is important to state that the thermal-induced unfolding of both full-length Hsp90α and C-Hsp90α were irreversible in the conditions tested here. Therefore, the discussion was centered only on the values of the Tms because of the difficulty in reliably measuring other thermodynamic parameters.

DSF experiments were performed using a fluorescent extrinsic probe (Spyro Orange dye) that recognizes hydrophobic sites in proteins. Then, when a protein is heated, hydrophobic patches are exposed and bind to the dye that fluoresces [42]. In the absence of celastrol, the thermal-induced unfolding profile of full-length Hsp90α by DSF had two distinct transitions with Tm values of 47.9 (named Tm_1) and 61.6 °C (named Tm_2) (Fig. S3A and Table 1), respectively, whereas C-Hsp90 had only one distinct transition with a Tm of 61.4 °C (Fig. S3B and Table 1). These results indicate that the two distinct Tms of full-length Hsp90α were mainly related to the unfolding of each of the two major domains of Hsp90α, the N- and C-terminal domains. Because the deletion mutant C-Hsp90α had a Tm of 61.4 °C, Tm_2 is very likely mainly related to the unfolding of the C-terminal domain, whereas Tm_1 is very likely mainly related to the unfolding of the N-terminal domain. Accordingly, studies using DSC to investigate the thermal-induced unfolding of a Hsp90 from the porcine brain (about 99% identical to human Hsp90α) also found two Tm values,

Table 1
Midpoint of the transition (Tm; in Celsius degrees) from thermal-induced unfolding profiles measured by DSF for C-Hsp90α and full-length Hsp90α.

Protein:celastrol	Hsp90α Tm_1 Tm_2	C-Hsp90α Tm
1:0	47.9 61.6	61.4
1:1	47.9 60.4	51.7
1:10	47.9 58.9	48.8

Errors are less than 2%.

Table 2
Midpoint of the transition (Tm; in Celsius degrees) from thermal-induced unfolding profiles measured by DSC for C-Hsp90α and full-length Hsp90α.

Protein:celastrol	Hsp90α Tm_1 Tm_2	C-Hsp90α Tm
1:0	48.2 66.2	64.2
1:1	48.0 65.3	62.0
1:2	–	59.8
1:4	47.5 64.7	–
1:10	46.9 59.0	–

Errors are less than 2%.

where the lower value was related to the unfolding of the N-terminal domain, and the higher value was related to the unfolding of the C-terminal domain [43]. The presence of celastrol affected the stability of full-length Hsp90α as indicated by the decrease in Tm_2 (from 61.6 °C in the absence of celastrol to 58.9 °C when ten-fold the concentration of celastrol was added) as the concentration of celastrol increased (Fig. S3A and Table 1) and by the observation that the same effect was detected when celastrol was added to C-Hsp90 (from 61.4 °C in the absence of celastrol to 48.8 °C when ten-fold the concentration of celastrol was added) (Fig. S3B and Table 1). These data strongly suggest that celastrol mainly affected the stability of the C-terminal domain as it affected Tm_2, but not Tm_1, of Hsp90α and the sole Tm of C-Hsp90α. The effect of celastrol appeared to be stronger on C-Hsp90α than on the full-length Hsp90α, and this difference may be due to stabilizing interactions between the N- and C-termini that are not affected by celastrol, but further investigation is need to verify the validity of this hypothesis.

The effect of celastrol on the stability of Hsp90α was also investigated by DSC, a technique widely used to determine the thermodynamic stability of proteins that measures the heat given off or absorbed excessively by the sample (protein in the case of this work) on the basis of temperature difference between the sample and the reference buffer [44]. In the absence of celastrol, the thermal-induced unfolding profile of full-length Hsp90α by DSC had two distinct transitions with Tm values of 48.2 °C (Tm_1) and 66.2 °C (Tm_2) (Fig. S4A and Table 2), respectively, whereas C-Hsp90α had only one distinct transition with a Tm of 64.2 °C (Fig. S4B and Table 2). It is noteworthy that, as discussed for the DSF data, the results using DSC also indicated that the two distinct Tm values of full-length Hsp90α were mainly related to the unfolding of each of the two major domains of Hsp90α, the N- and C-terminal domains. As the deletion mutant C-Hsp90α had a Tm of 64.2 °C (Table 2), Tm_2 is very likely mainly related to the unfolding of the C-terminal domain, whereas Tm_1 is very likely mainly related to the unfolding of the N-terminal domain. As also noticed by DSF, the presence of celastrol affects the stability of full-length Hsp90α, as shown by the decrease in Tm_2 as the concentration of celastrol increases (from 66.2 °C in the absence of celastrol to 59.0 °C when ten-fold the concentration of celastrol was added) (Table 2). The same effect was detected when celastrol was added to C-Hsp90α as Tm decreased from 64.2 °C in the absence of celastrol to 59.8 °C when two-fold the concentration of celastrol was added (Table 2). Because of the higher C-Hsp90α concentration required for reliable DSC thermograms, it was not technically possible to test high celastrol concentrations. Together, the thermodynamic data strongly suggest that celastrol directly targets Hsp90α and mainly affects the stability of the C-terminal domain as it affected Tm_2, but not Tm_1, and the sole Tm of C-Hsp90α. It is worth noting that the heat released upon unfolding of both the Hsp90 second transition and C-Hsp90α sole transition was drastically reduced, which also indicates the destabilization of the C-terminal domain. In addition, as measured by DSF, the DSC results indicated that the effect of celastrol is stronger on C-Hsp90α than on the full-length Hsp90α.

In both DSF and DSC experiments, celastrol decreased the Tm of unfolding, i.e., it acted as a destabilizer of Hsp90α (Fig. S5). These results are explained by a model in which the compound stabilizes, or at least have a larger stabilizing effect on, the unfolded state of Hsp90. In this model, in native conditions celastrol induces the oligomerization of Hsp90, and in denaturating conditions, where the oligomers unfold to monomers (see discussion below), these unfolded monomers are stabilized by celastrol. The explanation for ligand binding to denaturated states are supported by the fact that structured portions remain in proteins even in the presence of highly denaturing concentrations [45]. It is not straightforward to extrapolate these findings to in vivo conditions, but it is clear that celastrol at least disturbs the conformational equilibrium of Hsp90. That disturbance may be sufficient to perturb the function of Hsp90 chaperones in a tumorigenic cell. As previously discussed (see Introduction), tumor-purified Hsp90s are more susceptible to the effect of inhibitory compounds, and disturbing the conformation of Hsp90, as demonstrated above, may be the main action responsible for the antitumorigenic effect of celastrol.

3.2. Celastrol induced the oligomerization of Hsp90α via the C-terminal domain

The second finding of this work was that Hsp90α formed oligomers in the presence of celastrol and that the size of the oligomers was dependent on the concentration of the ligand. The size of proteins can be investigated with Dynamic Light Scattering (DLS), a well-established technique for measuring the size distribution profile of particles in solution. In the absence of celastrol, the main peak measured had a radius of 6.9 nm and 4.6 nm for full-length Hsp90α and C-Hsp90α, respectively (Table 2 and Fig. S6). The radius of approximately 4.6 nm of C-Hsp90α domain in the absence of celastrol corresponded to a particle with a mass of a dimer [43,46]. In the presence of increasing concentrations of celastrol, the DLS peak distribution of both full-length Hsp90α and C-Hsp90α displayed a significant shift toward high values, indicating an increasing size of the protein population distribution (Table 3). These results were confirmed by native PAGE, in which proteins were analyzed in non-denaturing conditions. In the absence of celastrol, the bands corresponding to both full-length Hsp90α and C-Hsp90α appeared in the gel with the expected masses of dimers (Fig. 1A and B, respectively). As the concentration of added celastrol increased, the band corresponding to the dimers had a lower intensity until the band faded to near non-existence (Fig. 1A and B). Surprisingly, bands corresponding to oligomers with higher molecular masses than dimers were not identified in the gel. The large size of the oligomers or modification of the pI may be possible explanations for these species not migrating into the gel, but these would need to be experimentally verified before further consideration.

To investigate the oligomerization process in more detail, we also performed multi-angle laser light-scattering experiments in line with size-exclusion chromatography (SEC–MALS). SEC–MALS is a nondestructive technique that allows the analysis of the native state of macromolecules in solution to determine the molecular mass with high precision. Fig. 2A shows the SEC–MALS results for C-Hsp90α in the absence and in the presence of celastrol at 1:2 stoichiometry. In the absence of celastrol, C-Hsp90α was eluted approximately 16 mL, with a measured molecular mass of approximately 44.8 kDa, which is in

Table 3
Radius (in nm) of the most intense peak measured by DLS for C-Hsp90α and full-length Hsp90α.

Protein:Celastrol	Hsp90α	C-Hsp90α
1:0	6.9	4.6
1:1	7.1	6.2
1:2	213.5	13.6
1:3	127.9 and 534.5*	16.7
1:4	–	138.5

* Two peaks of approximately the same intensity were identified; errors are less than 5%.

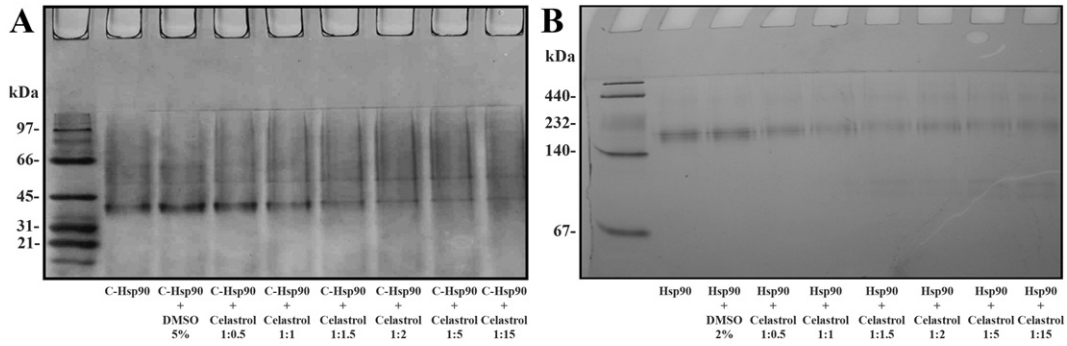

Fig. 1. Polyacrylamide gel electrophoresis at native conditions (native-PAGE) of full-length C-Hsp90α (A) and Hsp90α (B) in the absence and in the presence of increasing concentrations of celastrol. In the absence of celastrol, the bands corresponding to both full-length Hsp90α and C-Hsp90α appeared in the gel with the expected masses of dimers, but as the concentration of added celastrol increased, the band corresponding to dimers had lower intensity until almost disappearing. All experiments were performed using buffer Tris–HCl 20 mM, NaCl 150 mM, pH 7.4.

accordance with the theoretical mass of the dimer (43.7 kDa) (Fig. 2A). In the presence of celastrol (protein:celastrol molar ratio 1:2), C-Hsp90α was eluted approximately 10.5 mL with a measured molecular mass of approximately 207.0 kDa, which is almost identical to the mass of an oligomer formed by five dimers of C-Hsp90 (theoretical mass of 218.5 kDa) (Fig. 2A). SDS-PAGE of the samples loaded into SEC–MALS indicated that C-Hsp90α was present in the peaks (Fig. 2B). At a molar ratio of 1:3, the C-Hsp90α measured molecular mass was approximately 300.0 kDa, which is consistent with seven dimers of the C-Hsp90α (theoretical mass is 302.1 kDa) (Fig. S7). Taken together, these results clearly suggest that celastrol directly targeted Hsp90 and induced an oligomerization process via the C-terminal domain. It is noteworthy that the Hsp90α oligomers eluted from the column dissolved into monomers, even in the presence of celastrol, in the denaturing conditions of SDS-PAGE (Fig. 2B). Thus, these results strongly support our thermodynamic investigation indicating that the effect of celastrol is concentration dependent and that the compound disturbs the conformational equilibrium of Hsp90 (see above).

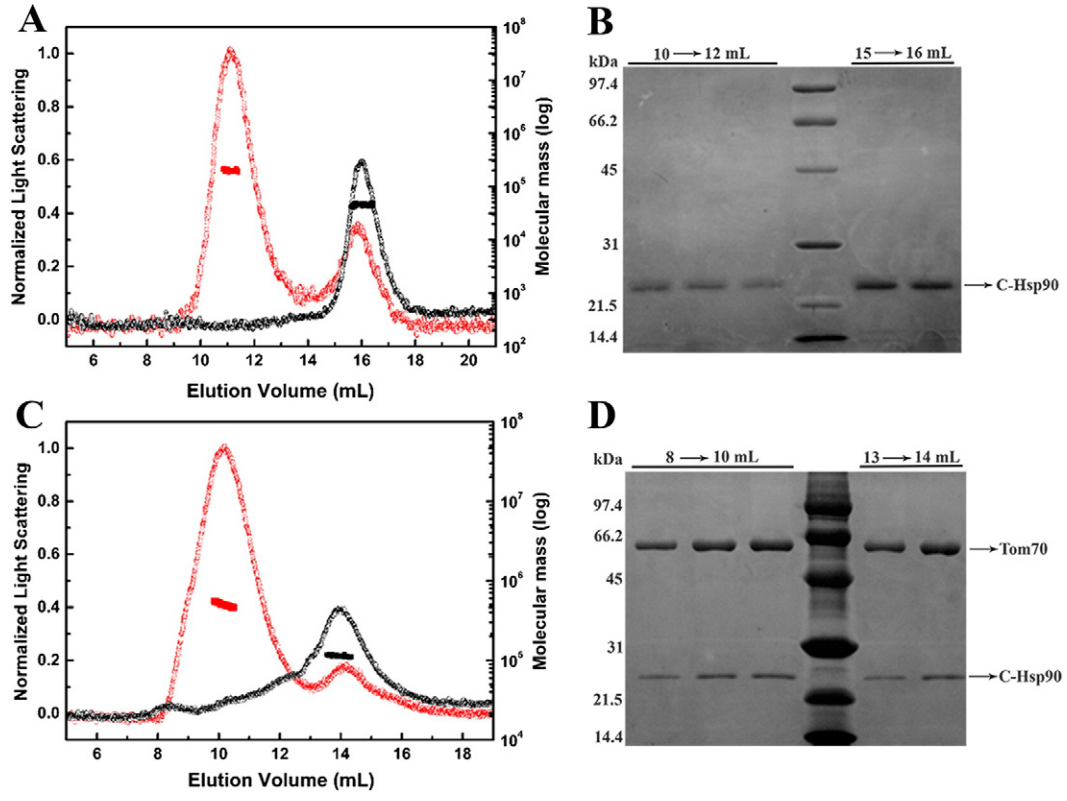

Fig. 2. A) SEC–MALS to determine the molecular mass of the C-Hsp90α in the presence and absence of celastrol (molar ratio 1:2; C-Hsp90:celastrol). The graph shows the profile of light scattering normalized and molecular mass distribution. In the absence of celastrol (open black circles), C-Hsp90α had a molecular mass of 44.8 kDa (closed black squares), which is consistent with the predicted molecular mass of a dimer, whereas in the presence of celastrol (open red circles), the C-Hsp90α had a molecular mass of 207.0 kDa (closed red squares), which is consistent with the molecular mass of 5 dimers. B) Samples collected in (A) were analyzed by SDS-PAGE that showed that C-Hsp90α was present in the peaks and that the chaperone unfolded to a monomer at the denaturant conditions of the gel, even in the presence of celastrol. C) SEC–MALS to determine the molecular mass of the C-Hsp90α/Tom70 complex in the presence and absence of celastrol (molar ratio 1:2; complex:celastrol). The figure shows normalized light scattering and molecular mass distribution. The C-Hsp90α/Tom70 complex in the absence of celastrol (open black circles) eluted with a molecular mass of 114.5 kDa (closed black squares), a result that is accordance with one dimer of C-Hsp90α domain bound to one monomer of Tom70 (theoretical mass is 103.6 kDa). When celastrol was added in a molar ratio of 1:2 (complex:celastrol), the complex eluted (open red circles) with a molecular mass of 527.2 kDa (closed red squares), a result that corresponded to five dimers of C-Hsp90α bound to five monomers of Tom70 (theoretical mass is 518.0 kDa). D) SDS-PAGE of the collected fractions from the SEC–MALS to confirm the presence of the bound proteins.

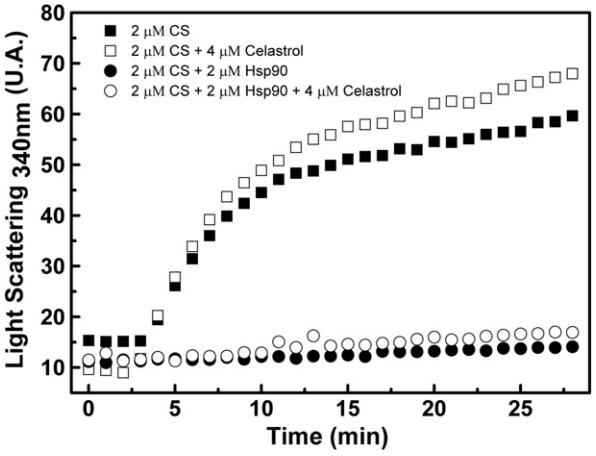

Fig. 3. Chaperone activity. Citrate synthase (CS; 2 μM) aggregated when heated at 45 °C as shown by scatter at 340 nm both in the absence (closed square) and in the presence (open square) of celastrol (4 uM). Incubation with Hsp90α (2 μM) prevented CS aggregation both in the absence (closed circles) and in the presence (open circles) of celastrol (4 uM).

3.3. The chaperone activity and the ability to bind a TPR co-chaperone was not affected by celastrol

Finally, we investigated the effect of celastrol on a couple of functional activities of Hsp90α. First, we tested whether celastrol affected the ability of Hsp90α to bind to co-chaperones with a TPR (tetratricopeptide repeat) domain, as this domain binds via a C-terminal MEEVD motif in Hsp90 [47], and celastrol appears to act primarily upon the C-terminal domain (see above). In a previous study, by combining SEC–MALS and calorimetry, we described that the stoichiometry of the interaction between the Hsp90 C-terminal domain and the TPR co-chaperone Tom70 is a dimer of the C-Hsp90 domain for one monomer of Tom70 [37]. Then, here, we investigated the effect of celastrol in the interaction between C-Hsp90α and Tom70 by SEC–MALS experiments. As previously demonstrated, the C-Hsp90/Tom70 complex in the absence of celastrol eluted with a molecular mass of approximately 114.5 kDa, a result that is in accordance with one dimer of the C-Hsp90α domain bound to one monomer of Tom70 (theoretical mass is 103.6 kDa) (Fig. 2C). When celastrol was added in a molar ratio of 1:2 (complex:celastrol), the complex eluted with a molecular mass of 527.2 kDa (Fig. 2C), which corresponds neatly to five dimers of C-Hsp90α bound to five monomers of Tom70 (theoretical mass is 518.0 kDa) (Fig. 2C). The presence of celastrol did not interfere with the formation of the complex as confirmed by SDS-PAGE of the peaks (Fig. 2D). In addition, the stoichiometry of interaction between C-Hsp90α and Tom70 was not altered in the presence of celastrol. In summary, although celastrol was able to modify the oligomeric state of the C-Hsp90α, it does not affect the binding with the co-chaperone Tom70.

We then asked whether celastrol would affect the ability of full-length Hsp90α (C-Hsp90 does not have this ability because it lacks the N-terminal domain) to protect proteins from aggregation. To that end, we used citrate synthase (CS), a protein that undergoes thermal aggregation and scatters light, as measured by absorbance at 340 nm [48], as a client of Hsp90, and the results are shown on Fig. 3. In the absence of full-length Hsp90α, CS started to aggregate after 5 min, and Hsp90α, at a molar ratio of 1:1, protected against aggregation (Fig. 3). The presence of celastrol did not alter the effect of Hsp90α, which was equally efficient in protecting against aggregation in the absence of the ligand, i.e., Hsp90α was still able to bind unfolded CS (Fig. 3).

4. Conclusions

A highly interesting conclusion from our work and others in the literature is that celastrol interferes with the specific biological functions of Hsp90. Results in this study suggest that Hsp90 will remain active in binding unfolded or partially unfolded protein clients in the presence of celastrol. There are also results that, together with published examples in the literature (see below), suggest that Hsp90 will bind only specific classes of co-chaperones (supported in this study and [31]). Thus, celastrol affects the actions of Hsp90 that depend on co-chaperones, the binding of which is perturbed/inhibited by celastrol [31, 34, this work]. Of course, one has to be careful to translate these findings to

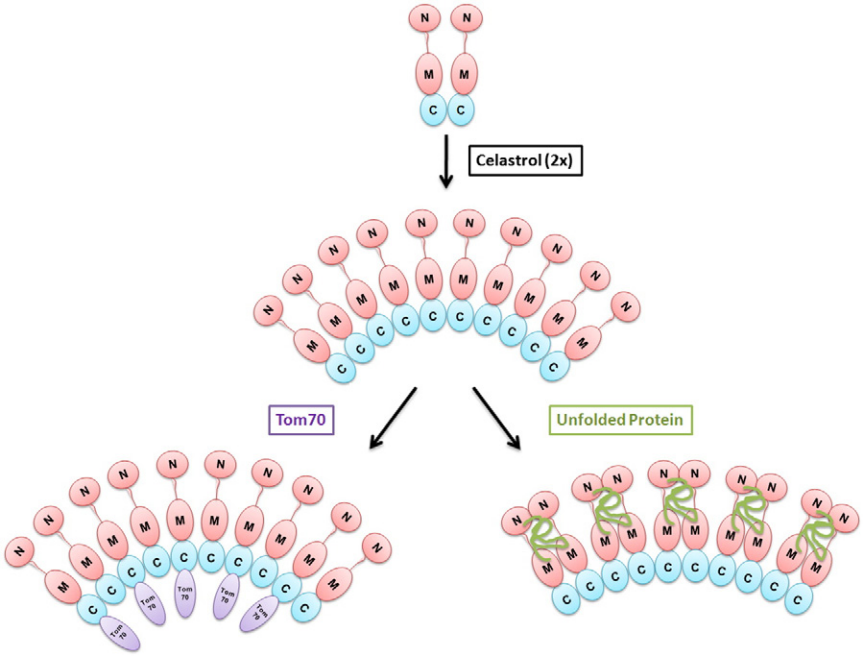

Fig. 4. Cartoon showing the effect that celastrol (2×) had on the oligomerization of Hsp90 and then on the interaction of Hsp90 with TOM70 and on the chaperone activity of Hsp90 based on the results of this manuscript.

the cell context as celastrol has other effects in the cell that do not depend on Hsp90 only, such as gene expression induction [49]. Moreover, we can suggest a model of action for the molecular interaction of celastrol with Hsp90 (Fig. 4). We suggest a model in which celastrol binds directly to the C-terminal domain of Hsp90 (supported by our results and that of [32]) but not the N-terminal domain (supported by [35] causing oligomerization (our results; Fig. 2C)). However, the ability to protect against protein aggregation (supported by our results) and to bind to TPR co-chaperones (supported by our results and [31]) are not affected by celastrol (Fig. 4). Because celastrol induces the oligomerization of p23 [34], a Hsp90 co-chaperone, we suggest that this ligand acts primarily by inducing specific oligomerization that affects some, but not all, of the functions of chaperones and co-chaperones. In addition, celastrol will act by disturbing the conformational equilibrium of Hsp90, shifting it toward unfolding in denaturating conditions, perhaps such conditions as those of a tumorigenic cell. Additionally, since Hsp90 is an intracellular inhibitor of HSF1 (Heat Shock Factor1) and a previous work reported that in vivo celastrol act stimulating HSF1 [29], one can suggest another hypothesis in which the oligomerization of Hsp90, as reported here, would result in an increase in the amount of functional HSF1 acting upon the expression of chaperone genes. A direct action of celastrol upon secreted Hsp90α that may be resulting in decreasing invasiveness should also be considered. Although these models warrant additional support, they suggest that the effect of celastrol may be subtle or at least more specific than previously suggested, and such an effect could be fine-tuned by modulating the concentration or by chemical modifications of the molecule. Thus, we hope that the findings of this manuscript may aid in the development of celastrol as an effective drug against cancers.

Conflict of interest

The authors declare that there is no conflict of interest.

Acknowledgments

We thank the Fundação de Amparo à Pesquisa do Estado de São Paulo (FAPESP) (2012/50161-8), Conselho Nacional de Pesquisa e Desenvolvimento (CNPq) (304426/2011-3), and Coordenação de Aperfeiçoamento de Pessoal de Nível Superior (CAPES) for their financial support and fellowships and CNPEM-LNBio for the use of facilities.

Appendix A. Supplementary data

Supplementary data to this article can be found online at http://dx.doi.org/10.1016/j.bbagen.2014.06.008.

References

[1] L. Neckers, Heat shock protein 90: the cancer chaperone, J. Biosci. 32 (2007) 517–530.
[2] L.M. Gava, C.H.I., Human 90 kDa heat shock protein Hsp90 as a target for cancer therapeutics, Curr. Chem. Biol. 3 (2009) 330–341.
[3] V.C. da Silva, C.H. Ramos, The network interaction of the human cytosolic 90 kDa heat shock protein Hsp90: a target for cancer therapeutics, J. Proteomics 75 (2012) 2790–2802.
[4] L. Whitesell, S. Santagata, N.U. Lin, Inhibiting Hsp90 to treat cancer: a strategy in evolution, Curr. Mol. Med. 12 (2012) 1108–1124.
[5] M.P. Mayer, B. Bukau, Molecular chaperones: the busy life of Hsp90, Curr. Biol. 9 (1999) R322–R325.
[6] J.C. Young, I. Moarefi, F.U. Hartl, Hsp90: a specialized but essential protein-folding tool, J. Cell Biol. 154 (2001) 267–273.
[7] S.E. Jackson, Hsp90: structure and function, Top. Curr. Chem. 328 (2013) 155–240.
[8] W.M. Obermann, H. Sondermann, A.A. Russo, N.P. Pavletich, F.U. Hartl, In vivo function of Hsp90 is dependent on ATP binding and ATP hydrolysis, J. Cell Biol. 143 (1998) 901–910.
[9] L. Whitesell, E.G. Mimnaugh, B. De Costa, C.E. Myers, L.M. Neckers, Inhibition of heat shock protein HSP90-pp60v-src heteroprotein complex formation by benzoquinone ansamycins: essential role for stress proteins in oncogenic transformation, Proc. Natl. Acad. Sci. U. S. A. 91 (1994) 8324–8328.
[10] S.M. Roe, C. Prodromou, R. O'Brien, J.E. Ladbury, P.W. Piper, L.H. Pearl, Structural basis for inhibition of the Hsp90 molecular chaperone by the antitumor antibiotics radicicol and geldanamycin, J. Med. Chem. 42 (1999) 260–266.
[11] S. Matsumoto, E. Tanaka, T.K. Nemoto, T. Ono, T. Takagi, J. Imai, Y. Kimura, I. Yahara, T. Kobayakawa, T. Ayuse, K. Oi, A. Mizuno, Interaction between the N-terminal and middle regions is essential for the in vivo function of HSP90 molecular chaperone, J. Biol. Chem. 277 (2002) 34959–34966.
[12] P. Meyer, C. Prodromou, B. Hu, C. Vaughan, S.M. Roe, B. Panaretou, P.W. Piper, L.H. Pearl, Structural and functional analysis of the middle segment of hsp90: implications for ATP hydrolysis and client protein and cochaperone interactions, Mol. Cell 11 (2003) 647–658.
[13] P. Hawle, M. Siepmann, A. Harst, M. Siderius, H.P. Reusch, W.M. Obermann, The middle domain of Hsp90 acts as a discriminator between different types of client proteins, Mol. Cell. Biol. 26 (2006) 8385–8395.
[14] C. Prodromou, G. Siligardi, R. O'Brien, D.N. Woolfson, L. Regan, B. Panaretou, J.E. Ladbury, P.W. Piper, L.H. Pearl, Regulation of Hsp90 ATPase activity by tetratricopeptide repeat (TPR)-domain co-chaperones, EMBO J. 18 (1999) 754–762.
[15] A.S. Sreedhar, C. Soti, P. Csermely, Inhibition of Hsp90: a new strategy for inhibiting protein kinases, Biochim. Biophys. Acta 1697 (2004) 233–242.
[16] A. Donnelly, B.S. Blagg, Novobiocin and additional inhibitors of the Hsp90 C-terminal nucleotide-binding pocket, Curr. Med. Chem. 15 (2008) 2702–2717.
[17] C.M. Palermo, C.A. Westlake, T.A. Gasiewicz, Epigallocatechin gallate inhibits aryl hydrocarbon receptor gene transcription through an indirect mechanism involving binding to a 90 kDa heat shock protein, Biochemistry 44 (2005) 5041–5052.
[18] E.A. Sausville, J.E. Tomaszewski, P. Ivy, Clinical development of 17-allylamino, 17-demethoxygeldanamycin, Curr. Cancer Drug Targets 3 (2003) 377–383.
[19] A. Kamal, L. Thao, J. Sensintaffar, L. Zhang, M.F. Boehm, L.C. Fritz, F.J. Burrows, A high-affinity conformation of Hsp90 confers tumour selectivity on Hsp90 inhibitors, Nature 425 (2003) 407–410.
[20] G. Chiosis, M.N. Timaul, B. Lucas, P.N. Munster, F.F. Zheng, L. Sepp-Lorenzino, N. Rosen, A small molecule designed to bind to the adenine nucleotide pocket of Hsp90 causes Her2 degradation and the growth arrest and differentiation of breast cancer cells, Chem. Biol. 8 (2001) 289–299.
[21] L. Neckers, Y. Lee, Cancer: the rules of attraction, Nature 425 (2003) 357–359.
[22] P. Workman, Altered states: selectively drugging the Hsp90 cancer chaperone, Trends Mol. Med. 10 (2004) 47–51.
[23] L. Neckers, Using natural product inhibitors to validate Hsp90 as a molecular target in cancer, Curr. Top. Med. Chem. 6 (2006) 1163–1171.
[24] D.B. Solit, G. Chiosis, Development and application of Hsp90 inhibitors, Drug Discov. Today 13 (2008) 38–43.
[25] W. Li, D. Sahu, F. Tsen, Secreted heat shock protein-90 (Hsp90) in wound healing and cancer, Biochim. Biophys. Acta 1823 (2012) 730–741.
[26] S.H. Millson, A.W. Truman, A. Racz, B. Hu, B. Panaretou, J. Nuttall, M. Mollapour, C. Soti, P.W. Piper, FEBS J. 274 (2007) 4453–4463.
[27] C.L. McDowell, R.B. Sutton, W.M.J. Obermann, Expression of Hsp90 chaperome proteins in human tumor tissue, Int. J. Biol. Macromol. 45 (2009) 310–314.
[28] A. Salminen, M. Lehtonen, T. Paimela, K. Kaarniranta, Celastrol: molecular targets of Thunder God Vine, Biochem. Biophys. Res. Commun. 394 (2010) 439–442.
[29] S.D. Westerheide, J.D. Bosman, B.N. Mbadugha, T.L. Kawahara, G. Matsumoto, S. Kim, W. Gu, J.P. Devlin, R.B. Silverman, R.I. Morimoto, Celastrols as inducers of the heat shock response and cytoprotection, J. Biol. Chem. 279 (2004) 56053–56060.
[30] H. Hieronymus, J. Lamb, K.N. Ross, X.P. Peng, C. Clement, A. Rodina, M. Nieto, J. Du, K. Stegmaier, S.M. Raj, K.N. Maloney, J. Clardy, W.C. Hahn, G. Chiosis, T.R. Golub, Gene expression signature-based chemical genomic prediction identifies a novel class of HSP90 pathway modulators, Cancer Cell 10 (2006) 321–330.
[31] T. Zhang, A. Hamza, X. Cao, B. Wang, S. Yu, C.G. Zhan, D. Sun, A novel Hsp90 inhibitor to disrupt Hsp90/Cdc37 complex against pancreatic cancer cells, Mol. Cancer Ther. 7 (2008) 162–170.
[32] T. Zhang, Y. Li, Y. Yu, P. Zou, Y. Jiang, D. Sun, Characterization of celastrol to inhibit hsp90 and cdc37 interaction, J. Biol. Chem. 284 (2009) 35381–35389.
[33] B. Peng, L. Xu, F. Cao, T. Wei, C. Yang, G. Uzan, D. Zhang, HSP90 inhibitor, celastrol, arrests human monocytic leukemia cell U937 at G0/G1 in thiol-containing agents reversible way, Mol. Cancer 9 (2010) 79.
[34] A. Chadli, S.J. Felts, Q. Wang, W.P. Sullivan, M.V. Botuyan, A. Fauq, M. Ramirez-Alvarado, G. Mer, Celastrol inhibits Hsp90 chaperoning of steroid receptors by inducing fibrillization of the Co-chaperone p23, J. Biol. Chem. 285 (2010) 4224–4231.
[35] S. Sreeramulu, S.L. Gande, M. Gobel, H. Schwalbe, Molecular mechanism of inhibition of the human protein complex Hsp90–Cdc37, a kinome chaperone–cochaperone, by triterpene celastrol, Angew. Chem. Int. Ed. Engl. 48 (2009) 5853–5855.
[36] D. Zhang, L. Xu, F. Cao, T. Wei, C. Yang, G. Uzan, B. Peng, Celastrol regulates multiple nuclear transcription factors belonging to HSP90's clients in a dose- and cell type-dependent way, Cell Stress Chaperones 15 (2010) 939–946.
[37] L.M. Gava, D.C. Goncalves, J.C. Borges, C.H. Ramos, Stoichiometry and thermodynamics of the interaction between the C-terminus of human 90 kDa heat shock protein Hsp90 and the mitochondrial translocase of outer membrane Tom70, Arch. Biochem. Biophys. 513 (2011) 119–125.
[38] D.H.A. Correa, C.H.I. Ramos, The use of circular dichroism spectroscopy to study protein folding, form and function, Afr. J. Biochem. Res. 3 (5) (2009) 164–173.
[39] U.B. Ericsson, B.M. Hallberg, G.T. Detitta, N. Dekker, P. Nordlund, Thermofluor-based high-throughput stability optimization of proteins for structural studies, Anal. Biochem. 357 (2006) 289–298.
[40] D.E. Bollag, M.D. Rozycki, S.J. Edelstein, Protein methods, second ed., 1996.

[41] C.H. Ramos, S.T. Ferreira, Protein folding, misfolding and aggregation: evolving concepts and conformational diseases, Protein Pept. Lett. 12 (2005) 213–222.
[42] F.H. Niesen, H. Berglund, M. Vedadi, The use of differential scanning fluorimetry to detect ligand interactions that promote protein stability, Nat. Protoc. 2 (2007) 2212–2221.
[43] C. Garnier, D. Lafitte, P.O. Tsvetkov, P. Barbier, J. Leclerc-Devin, J.M. Millot, C. Briand, A.A. Makarov, M.G. Catelli, V. Peyrot, Binding of ATP to heat shock protein 90: evidence for an ATP-binding site in the C-terminal domain, J. Biol. Chem. 277 (2002) 12208–12214.
[44] M.M. Lopez, G.I. Makhatadze, Differential scanning calorimetry, Methods Mol. Biol. 173 (2002) 113–119.
[45] M.A. Lietzow, M. Jamin, H.J. Dyson, P.E. Wright, Mapping long-range contacts in a highly unfolded protein, J. Mol. Biol. 322 (2002) 655–662.
[46] C. Garnier, P. Barbier, F. Devred, G. Rivas, V. Peyrot, Hydrodynamic properties and quaternary structure of the 90 kDa heat-shock protein: effects of divalent cations, Biochemistry 41 (2002) 11770–11778.
[47] A. Brinker, C. Scheufler, F. von der Mulbe, B. Fleckenstein, C. Herrmann, G. Jung, I. Moarefi, F.U. Hartl, Ligand discrimination by TPR domains — relevance and selectivity of EEVD-recognition in Hsp70 center dot Hop center dot Hsp90 complexes, J. Biol. Chem. 277 (2002) 19265–19275.
[48] U. Jakob, H. Lilie, I. Meyer, J. Buchner, Transient interaction of Hsp90 with early unfolding intermediates of citrate synthase. Implications for heat shock in vivo, J. Biol. Chem. 270 (1995) 7288–7294.
[49] C. Yang, C.L. Swallows, C. Zhang, J. Lu, H. Xiao, R.O. Brady, Z. Zhuang, Celastrol increases glucocerebrosidase activity in Gaucher disease by modulating molecular chaperones, Proc. Natl. Acad. Sci. U. S. A. 111 (2014) 249–254.